Endocannabinoid Hydrolysis Generates Brain Prostaglandins That Promote Neuroinflammation

Daniel K. Nomura, *et al.*

Science **334**, 809 (2011);
DOI: 10.1126/science.1209200

Table 1. The kinetic parameters of Sirt5 on acetyl, malonyl, and succinyl peptides with different sequences. ND, cannot be determined either because no activity was observed or because initial rate (V) versus substrate concentration ([S]) was linear (even the highest [S] of 750 μM used was much smaller than the K_m).

Peptide	k_{cat} (s^{-1})	K_m for peptide (μM)	k_{cat}/K_m (s^{-1} M^{-1})
H3 K9			
(4–13 + WW*)			
Deacetylation	ND	ND (>750)	7.8
Demalonylation	0.037 ± 0.003	6.1 ± 2.8	6.1×10^3
Desuccinylation	0.025 ± 0.002	5.8 ± 2.7	4.3×10^3
GDH K503			
(498–509 + WW*)			
Deacetylation	ND	ND (>750)	<2†
Demalonylation	0.014 ± 0.001	8.7 ± 1.3	1.6×10^3
Desuccinylation	0.028 ± 0.002	14 ± 4	2.0×10^3
ACS2 K628			
(623-632 + WW*)			
Deacetylation	ND	ND (>750)	18
Demalonylation	0.079 ± 0.008	150 ± 40	5.2×10^2
Desuccinylation	0.268 ± 0.051	450 ± 150	6.0×10^2

*Two tryptophan residues were added at the C-terminal of the peptide to facilitate the detection with ultraviolet-visible light absorption during the high-performance liquid chromatography assay. †No activity. The value was estimated on the basis of the detection limit.

Acetylation occurs on numerous metabolic enzymes and regulates their activities in mammals and bacteria (*24*, *25*). Given that succinyl-CoA and malonyl-CoA are common metabolites like acetyl-CoA (*14*), and all the succinylated and malonylated proteins we found are metabolic enzymes, it is likely that protein lysine succinylation and malonylation function similarly to acetylation and regulate metabolism (*24*, *25*).

References and Notes

1. A. A. Sauve, C. Wolberger, V. L. Schramm, J. D. Boeke, *Annu. Rev. Biochem.* **75**, 435 (2006).
2. S.-i. Imai, L. Guarente, *Trends Pharmacol. Sci.* **31**, 212 (2010).
3. M. C. Haigis, D. A. Sinclair, *Annu. Rev. Pathol.* **5**, 253 (2010).
4. S.-i. Imai, C. M. Armstrong, M. Kaeberlein, L. Guarente, *Nature* **403**, 795 (2000).
5. K. G. Tanner, J. Landry, R. Sternglanz, J. M. Denu, *Proc. Natl. Acad. Sci. U.S.A.* **97**, 14178 (2000).
6. R. A. Frye, *Biochem. Biophys. Res. Commun.* **273**, 793 (2000).
7. E. Michishita, J. Y. Park, J. M. Burneskis, J. C. Barrett, I. Horikawa, *Mol. Biol. Cell* **16**, 4623 (2005).
8. M. C. Haigis *et al.*, *Cell* **126**, 941 (2006).
9. A. Schuetz *et al.*, *Structure* **15**, 377 (2007).
10. G. Liszt, E. Ford, M. Kurtev, L. Guarente, *J. Biol. Chem.* **280**, 21313 (2005).
11. E. Michishita *et al.*, *Nature* **452**, 492 (2008).
12. M. S. Cosgrove *et al.*, *Biochemistry* **45**, 7511 (2006).
13. K. G. Hoff, J. L. Avalos, K. Sens, C. Wolberger, *Structure* **14**, 1231 (2006).
14. L. Gao *et al.*, *J. Chromatogr. B Analyt. Technol. Biomed. Life Sci.* **853**, 303 (2007).
15. K.-H. Kim, *Annu. Rev. Nutr.* **17**, 77 (1997).
16. D. Saggerson, *Annu. Rev. Nutr.* **28**, 253 (2008).
17. A. A. Sauve *et al.*, *Biochemistry* **40**, 15456 (2001).
18. B. C. Smith, J. M. Denu, *Biochemistry* **45**, 272 (2006).
19. B. C. Smith, J. M. Denu, *Biochemistry* **46**, 14478 (2007).
20. W. F. Hawse *et al.*, *Structure* **16**, 1368 (2008).
21. R. Rosen *et al.*, *FEBS Lett.* **577**, 386 (2004).
22. T. Nakagawa, D. J. Lomb, M. C. Haigis, L. Guarente, *Cell* **137**, 560 (2009).
23. Z. Zhang *et al.*, *Nat. Chem. Biol.* **7**, 58 (2011).
24. S. Zhao *et al.*, *Science* **327**, 1000 (2010).
25. Q. Wang *et al.*, *Science* **327**, 1004 (2010).

Acknowledgments. This work is supported in part by Dreyfus Foundation (H.L.); grants NIH R01GM086703 (H.L.), Hong Kong GRF766510 (Q.H.), NIH RR01646 (R.A.C. and Q.H.), and NIH PPG DK58920 (J.A.); the European Union Ideas program (sirtuins; ERC-2008-AdG-23118 to J.A.); and the Ecole Polytechnique Fédérale de Lausanne (J.A.). Atomic coordinates and structure factors were deposited in the Protein Data Bank (accession codes 3RIG and 3RIY).

Supporting Online Material

www.sciencemag.org/cgi/content/full/334/6057/806/DC1
Materials and Methods
Figs. S1 to S17
Tables S1 to S7
References (*26*–*32*)

3 May 2011; accepted 23 September 2011
10.1126/science.1207861

Endocannabinoid Hydrolysis Generates Brain Prostaglandins That Promote Neuroinflammation

Daniel K. Nomura,[1,2]*† Bradley E. Morrison,[3]* Jacqueline L. Blankman,[1] Jonathan Z. Long,[1] Steven G. Kinsey,[4] Maria Cecilia G. Marcondes,[3] Anna M. Ward,[1] Yun Kyung Hahn,[5] Aron H. Lichtman,[5] Bruno Conti,[3] Benjamin F. Cravatt[1]*†

Phospholipase A_2(PLA_2) enzymes are considered the primary source of arachidonic acid for cyclooxygenase (COX)–mediated biosynthesis of prostaglandins. Here, we show that a distinct pathway exists in brain, where monoacylglycerol lipase (MAGL) hydrolyzes the endocannabinoid 2-arachidonoylglycerol to generate a major arachidonate precursor pool for neuroinflammatory prostaglandins. MAGL-disrupted animals show neuroprotection in a parkinsonian mouse model. These animals are spared the hemorrhaging caused by COX inhibitors in the gut, where prostaglandins are instead regulated by cytosolic PLA_2. These findings identify MAGL as a distinct metabolic node that couples endocannabinoid to prostaglandin signaling networks in the nervous system and suggest that inhibition of this enzyme may be a new and potentially safer way to suppress the proinflammatory cascades that underlie neurodegenerative disorders.

Inflammation is a hallmark of many neurological disorders, including chronic pain, traumatic brain injury, neurodegenerative diseases, and stroke (*1*). Prominent among the known proinflammatory stimuli in the nervous system are prostaglandins, which are produced by cyclooxygenase enzymes (COX1 and COX2) (*2*) that are in neurons and glial cells (*3*). Rodents treated with COX inhibitors or lacking COX enzymes show protection in models of neurodegenerative disorders that have an inflammatory component such as Parkinson's and Alzheimer's disease (*4*–*6*). However, the gastrointestinal and cardiovascular toxicities displayed by COX inhibitors have limited their translational potential for neuroinflammatory syndromes (*7*, *8*).

Phospholipase A_2 (PLA_2) enzymes, and cytosolic PLA_2 ($cPLA_2$ or *Pla2g4a*) in particular, have been viewed as the principal source of

[1]The Skaggs Institute for Chemical Biology and Department of Chemical Physiology, The Scripps Research Institute, 10550 North Torrey Pines Road, La Jolla, CA 92037, USA. [2]Program in Metabolic Biology, Department of Nutritional Sciences and Toxicology, University of California, Berkeley, 127 Morgan Hall, Berkeley, CA 94720, USA. [3]Molecular and Integrative Neurosciences Department, The Scripps Research Institute, 10550 North Torrey Pines Road, La Jolla, CA 92037, USA. [4]Department of Psychology, West Virginia University, Post Office Box 6040, Morgantown, WV 26506, USA. [5]Department of Pharmacology and Toxicology, Medical College of Virginia Campus, Virginia Commonwealth University, Richmond, VA 23298, USA.

*These authors contributed equally to this work.
†To whom correspondence should be addressed. E-mail: dnomura@berkeley.edu (D.K.N.) cravatt@scripps.edu (B.F.C.)

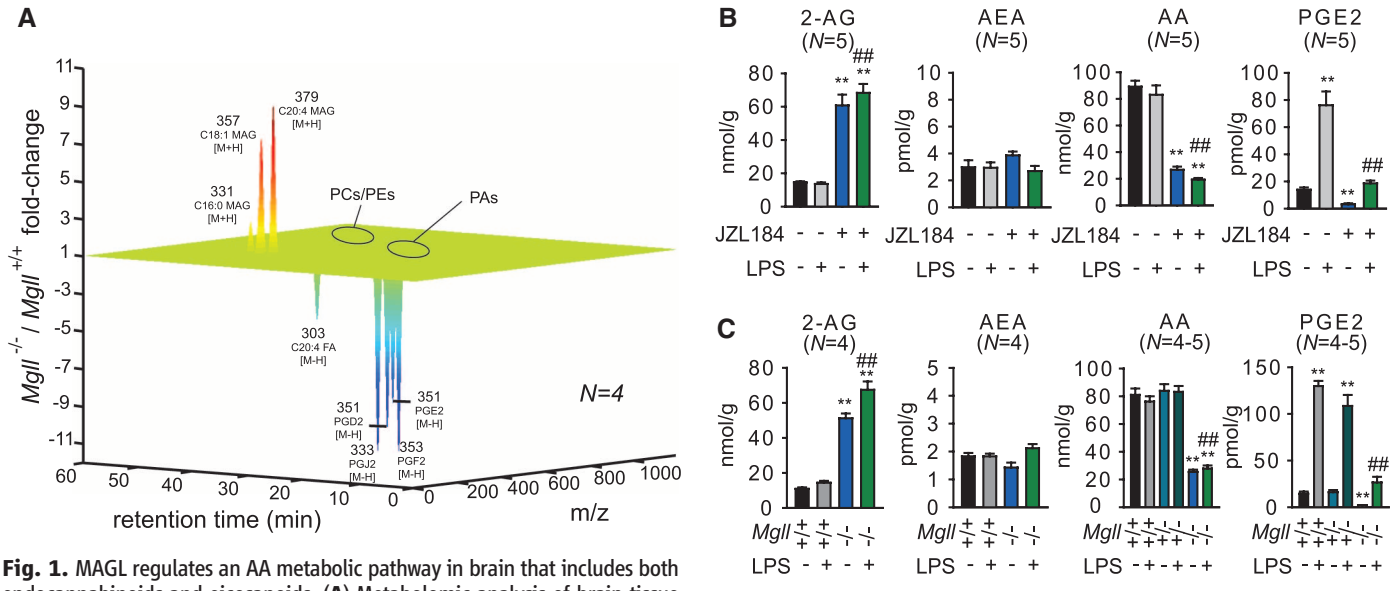

Fig. 1. MAGL regulates an AA metabolic pathway in brain that includes both endocannabinoids and eicosanoids. (**A**) Metabolomic analysis of brain tissue from *Mgll*$^{+/+}$ and *Mgll*$^{-/-}$ mice. Organic extracts of *Mgll*$^{+/+}$ and *Mgll*$^{-/-}$ brains were analyzed by liquid chromatography–mass spectrometry (LC-MS) in both the positive and negative ion mode by scanning a broad mass range for mass/charge ratio (*m/z*) values between 100 and 1200. Metabolite levels that showed a least a twofold difference between *Mgll*$^{+/+}$ and *Mgll*$^{-/-}$ brains (with *P* values of <0.05) were determined by the software program XCMS (*30*), and these differences were confirmed by manual quantification of extracted ion peaks. Metabolites altered less than twofold are not included in the metabolomics plot. Abbreviations: phosphatidylcholine (PCs), phosphatidylethanolamines (PEs), and phosphatidic acids (PAs). Eicosanoids, which are too low in abundance for detection in brain tissue by untargeted mass scanning, were measured by targeted selected reaction monitoring. (**B**) Brain metabolite levels (determined by selected reaction monitoring using LC-MS) from mice treated with the MAGL inhibitor JZL184 (40 mg/kg, i.p.) or vehicle 30 min before administration of LPS (20 mg/kg, i.p., 6 hours) or vehicle. (**C**) Brain metabolite levels from *Mgll*$^{+/+}$, $^{+/-}$, and $^{-/-}$ mice with or without LPS treatment (20 mg/kg, i.p., 6 hours). *$P < 0.05$ and **$P < 0.01$ for LPS-treated, JZL184-treated, or *Mgll*$^{-/-}$ groups compared with vehicle or *Mgll*$^{+/+}$ group. ##$P <$ 0.01 for JZL184/LPS-treated versus LPS-treated groups, or LPS-treated *Mgll*$^{-/-}$ versus LPS-treated *Mgll*$^{+/+}$ or *Mgll*$^{+/-}$ groups. No statistically significant differences were observed between *Mgll*$^{+/-}$ and $^{+/+}$ groups. Data shown are from mice killed by rapid decapitation (*16*). Similar results were obtained with mice killed by head-focused microwave irradiation, although the absolute brain levels of AA and prostaglandins in these animals were 1/5th to 1/20th those of the decapitated mice. (fig. S2) (*17*). Data are means ± SEM; $N = 4$ to 5 mice per group. Experiments were performed twice, and one data set is shown.

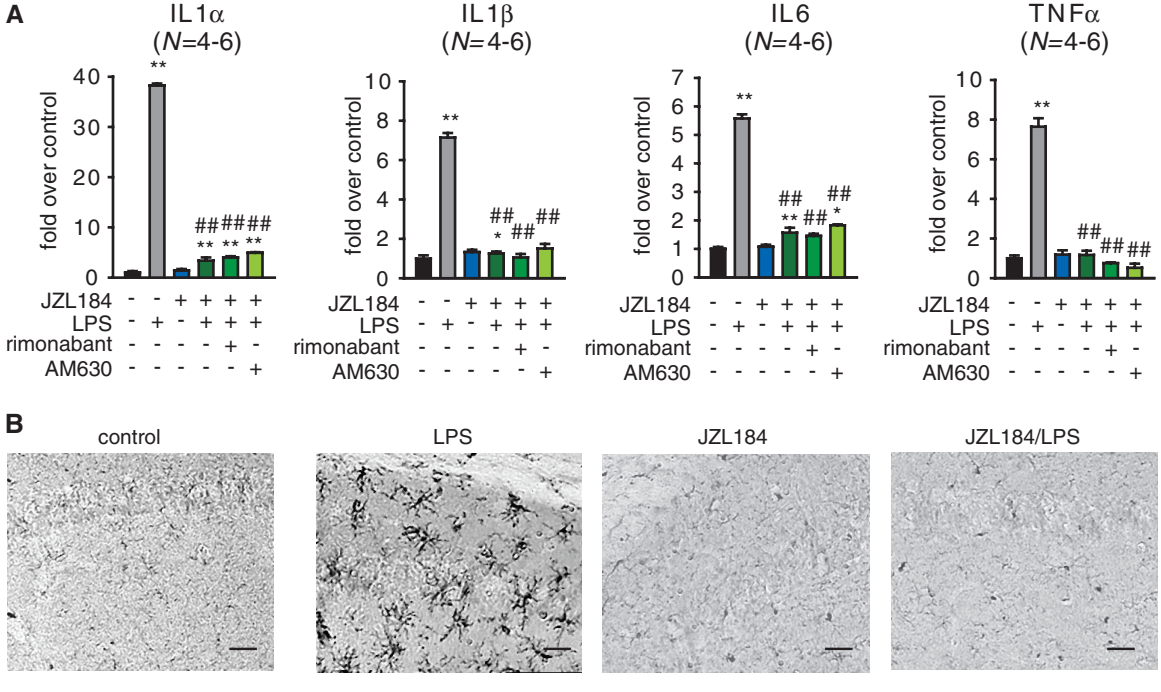

Fig. 2. MAGL blockade impairs LPS-induced neuroinflammatory responses in the mouse brain. (**A**) Inflammatory cytokine levels as measured by quantitative enzyme-linked immunosorbent assay in brain tissue from mice treated with JZL184 (40 mg/kg, i.p.) or vehicle administered 30 min before vehicle or LPS treatment (20 mg/kg i.p., 6 hours). The CB1 and CB2 antagonists rimonabant (1 mg/kg) and AM630 (1 mg/kg), respectively, were administered i.p. 30 min before JZL184 treatment. (**B**) Microglial activation assessed by Iba-1 staining (Iba-1 is a marker of microglial cells and is up-regulated on activation of microglia) of hippocampal regions from LPS-treated (20 μg in 100 μl phosphate-buffered saline injected i.p. once per day for 4 days) or vehicle-treated mice administered vehicle or JZL184 (40 mg/kg, oral gavage, once per day for 4 days). Images were taken at 20× on a bright-field microscope. Panels in (B) are the same magnification; scale bars, 50 μm. *$P < 0.05$, **$P < 0.01$ for all groups compared with vehicle-treated control mice (A). ##$P < 0.01$ for JZL184, rimonabant, and/or AM630-treated LPS-treated groups versus vehicle LPS-treated groups. Data are means ± SEM; $N = 4$ to 6 mice per group. Experiments were performed twice, and data sets were pooled for (A). A representative data set is shown for (B).

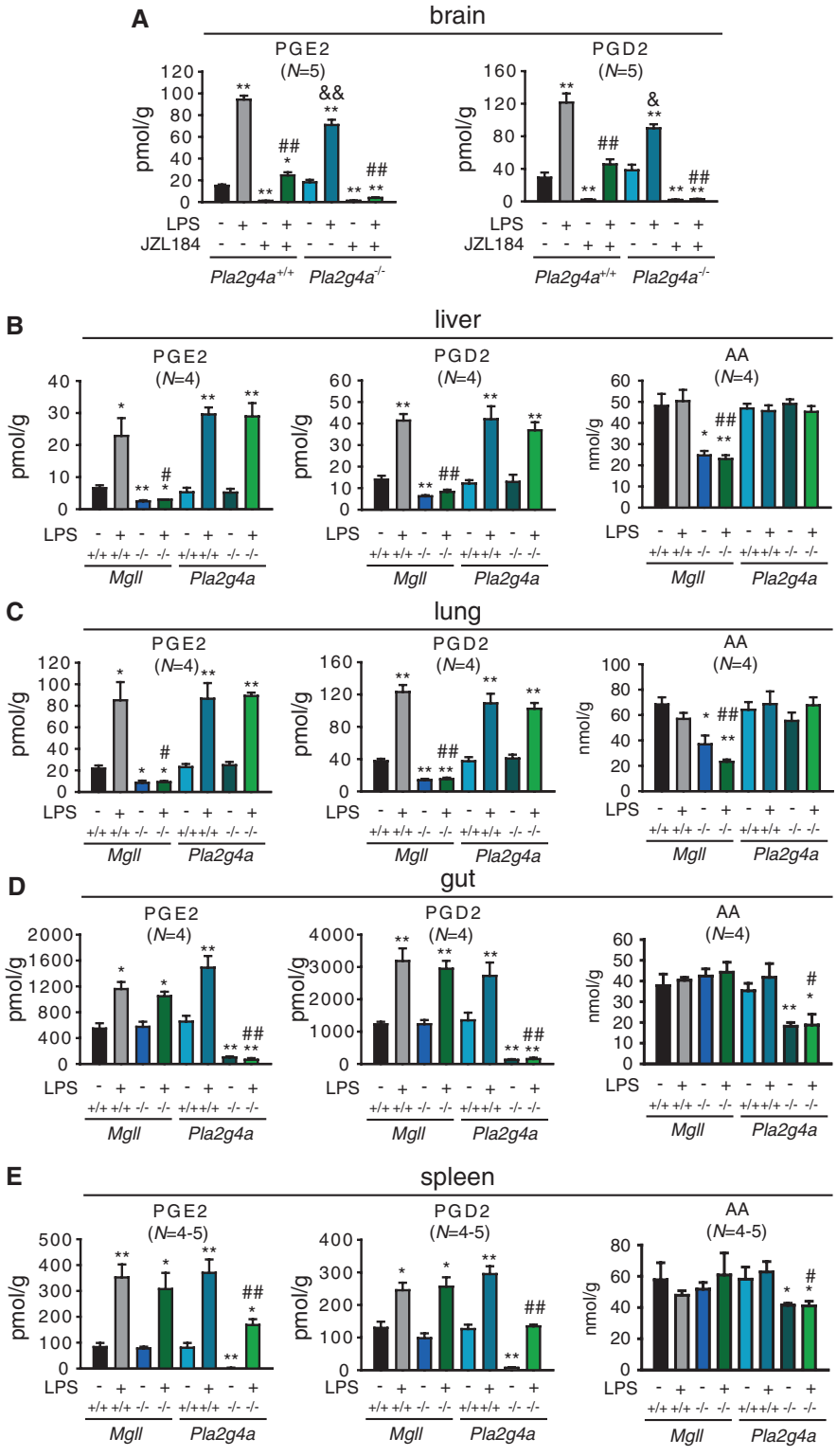

Fig. 3. Anatomical portrait of the contributions that MAGL and $cPLA_2$ make to eicosanoid metabolism in mice. (**A**) Brain metabolite levels determined by single-ion monitoring by LC-MS from *Pla2g4a*$^{+/+}$ and $^{-/-}$ mice treated with JZL184 (40 mg/kg, i.p.) or vehicle 30 min before administration of LPS (20 mg/kg i.p., 6 hours) or vehicle. (**B** to **E**), Metabolite levels in liver (B), lung (C), gut (D) and spleen (E) tissue from *Mgll*$^{+/+}$, *Mgll*$^{-/-}$, *Pla2g4a*$^{+/+}$, and *Pla2g4a*$^{-/-}$ mice after administration of LPS (20 mg/kg i.p., 6 hours) or vehicle. $^{**}P < 0.01$ for all groups compared with the vehicle-treated *Pla2g4a*$^{+/+}$ group in (A), and *Mgll*$^{-/-}$ versus *Mgll*$^{+/+}$ groups or *Pla2g4a*$^{-/-}$ versus *Pla2g4a*$^{+/+}$ groups for (B). $\#\#P < 0.01$ for *Pla2g4a*$^{+/+}$ or *Pla2g4a*$^{-/-}$ groups treated with JZL184 and/or LPS versus the *Pla2g4a*$^{+/+}$ group treated with vehicle and/or LPS. $\&\&P < 0.01$ for *Pla2g4a*$^{-/-}$ mice treated with LPS versus *Pla2g4a*$^{+/+}$ mice treated with LPS. Data are means ± SEM; N = 4 to 5 mice per group. Experiments were performed twice, and one representative data set is shown.

arachidonic acid (AA) for COX-mediated prostaglandin production (*9*); however, $cPLA_2$-deficient mice have unaltered AA levels in brain (*10*). This finding, coupled with our recent observation that the genetic or pharmacological inactivation of monoacylglycerol lipase (MAGL, *Mgll*) in mice causes significant reductions in brain AA (*11*–*13*), led us to investigate the potential existence of non-PLA_2 mechanisms that regulate prostaglandin production in the nervous system.

MAGL has been studied mostly for its role in hydrolyzing the endocannabinoid 2-arachidonoylglycerol (2-AG) (*11*, *14*, *15*). Consistent with previous investigations, we found that mice deficient in the gene that encodes MAGL (*Mgll*$^{-/-}$ mice) or mice treated with the MAGL-selective inhibitor JZL184 [40 mg/kg, intraperitoneally (i.p.)] showed loss of MAGL activity (*11*, *12*), but not other brain serine hydrolase activities (fig. S1, A and B), and had elevated brain levels of 2-AG and corresponding reductions in AA (Fig. 1, A to C) (*16*) (table S1). We more broadly profiled the metabolomic effects of MAGL disruption, using a combination of targeted and untargeted metabolomic approaches, and discovered by targeted analysis that inactivation of this enzyme also caused significant reductions in several prostaglandins and other eicosanoids in the brain, including prostaglandin E_2 (PGE_2), PGD_2, PGF_2, and thromboxane B2 (TXB2) (Fig. 1, A to C, and fig. S2A) (*17*). In contrast, other arachidonoyl-containing phospho- and neutral lipid species—including the second major endocannabinoid anandamide (*N*-arachidonoylethanolamide), as well as other free fatty acids—were unaltered in brain tissue from MAGL-deficient animals (Fig. 1, A to C, and fig. S3). These results indicate that the principal metabolic effects of disrupting MAGL in the brain are elevations in substrate MAGs, including 2-AG, and reductions in the product AA and downstream AA-derived eicosanoids.

We next asked whether MAGL also controls eicosanoid production in states of neuroinflammation. Mice were systemically administered the proinflammatory agent lipopolysaccharide (LPS) (*18*) (20 mg/kg i.p.) for 2 to 6 hours, then animals were killed and their brain lipids measured. LPS treatment produced a robust, time-dependent increase in brain eicosanoids (Fig. 1, B and C, and fig. S2, A and C), and these changes were markedly blunted in mice treated with JZL184 (Fig. 1B and fig. S2A) and in *Mgll*$^{-/-}$ mice (Fig. 1C and fig. S2A). Eicosanoids did rise substantially in brains from LPS-treated mice lacking MAGL; however, their levels did not significantly exceed the basal levels observed in untreated wild-type mice (Fig. 1, B and C, and figs. S2A and S4A). The impairment in brain eicosanoid production in MAGL-deficient animals was not reversed by cannabinoid receptor type 1 (CB1, *CNR1*) or type 2 (CB2, *CNR2*) antagonists rimonabant and AM630, respectively (1 mg/kg, administered i.p. 30 min before JZL184) or in *Cnr1*/*Cnr2* $^{-/-}$

mice (fig. S4B), which strengthened our conclusion that this metabolic effect is a direct consequence of reductions in AA rather than an indirect consequence of enhanced endocannabinoid signaling. COX1-selective (by SC560), but not COX2-selective (by celecoxib) inhibition, reduced both basal and LPS-induced brain prostaglandin levels, which mirrored the metabolic effects caused by MAGL inactivation (fig. S4C). We also noted that LPS treatment did not alter brain AA levels, despite causing elevations in prostaglandins. This finding could be explained in the context of previous reports showing that LPS induces COX1 expression in the brain (*19*). A model thus emerges where LPS-induced COX1 shunts a small proportion of the high bulk levels of AA (20 to 100 nmol/g brain weight) toward prostaglandins, which are found at much lower levels in brain (1 to 100 pmol/g brain weight). By controlling the quantity of AA available to LPS-induced COX1, MAGL exerts a crucial control over brain prostaglandin production in both basal and neuroinflammatory states.

LPS treatment induces widespread elevations in proinflammatory cytokines, including interleukin-1α (IL-1α), IL-1β, IL-6, and tumor necrosis factor α (TNFα) (*20*). We found that pharmacological or genetic inactivation of MAGL, although not affecting basal cytokine levels, produced a near-complete blockade of LPS-induced elevations in brain cytokines (Fig. 2A and fig. S5A). This suppression of cytokines was not reversed by CB1 or CB2 antagonists or in *Cnr1/Cnr2*$^{-/-}$ mice (Fig. 2A and fig. S5B). Disruption of MAGL also blocked LPS-induced microglial activation (Fig. 2B and fig. S5, C and D). SC-560 also reduced LPS-stimulated cytokine production in the brain, whereas celecoxib paradoxically further increased IL-1α and IL-1β levels in LPS-treated animals (fig. S6). These results are consistent with recent studies showing that mice deficient in COX1 and COX2 display attenuated and exacerbated neuroinflammatory responses to LPS-treatment, respectively (*2*, *20*, *21*).

Because previous studies have provided evidence that $cPLA_2$ also plays a role in prostaglandin production and neuroinflammation (*10*, *22*–*24*), we sought to assess the relative contributions of MAGL and $cPLA_2$ to brain prostaglandin generation. As has been reported previously (*10*, *22*), we found that the basal levels of AA and prostaglandins—as well as general serine hydrolase activities, including MAGL—were unaltered in brain tissue from mice deficient in $cPLA_2$ (*Pla2g4a*$^{-/-}$ mice) (*25*) (Fig. 3A and fig. S7, A and B). A modest, but significant, reduction (~20%) in LPS-induced prostaglandins was, however, detected in brains from *Pla2g4a*$^{-/-}$ mice (Fig. 3A), consistent with past findings (*22*). This reduction in brain prostaglandins was much lower in magnitude than the decrease observed in MAGL-deficient animals. Note that the effects of MAGL and $cPLA_2$ blockade were additive: Treatment with JZL184 produced greater reductions in brain prostaglandins in LPS-treated *Pla2g4a*$^{-/-}$ mice than in LPS-treated *Pla2g4a*$^{+/+}$ mice (Fig. 3A). These data indicate that both MAGL and $cPLA_2$ contribute to the AA pools for neuroinflammatory prostaglandins, such that the combined inactivation of these enzymes completely blocks brain prostaglandin increases caused by LPS.

Intrigued by the different roles played by MAGL and $cPLA_2$ in the brain, we expanded our analysis of these enzymes' contributions to prostaglandin metabolism to peripheral tissues. A clear partitioning of function was uncovered, with MAGL exerting control over both basal and LPS-induced AA and prostaglandins in liver and lung (Fig. 3, B and C), whereas $cPLA_2$

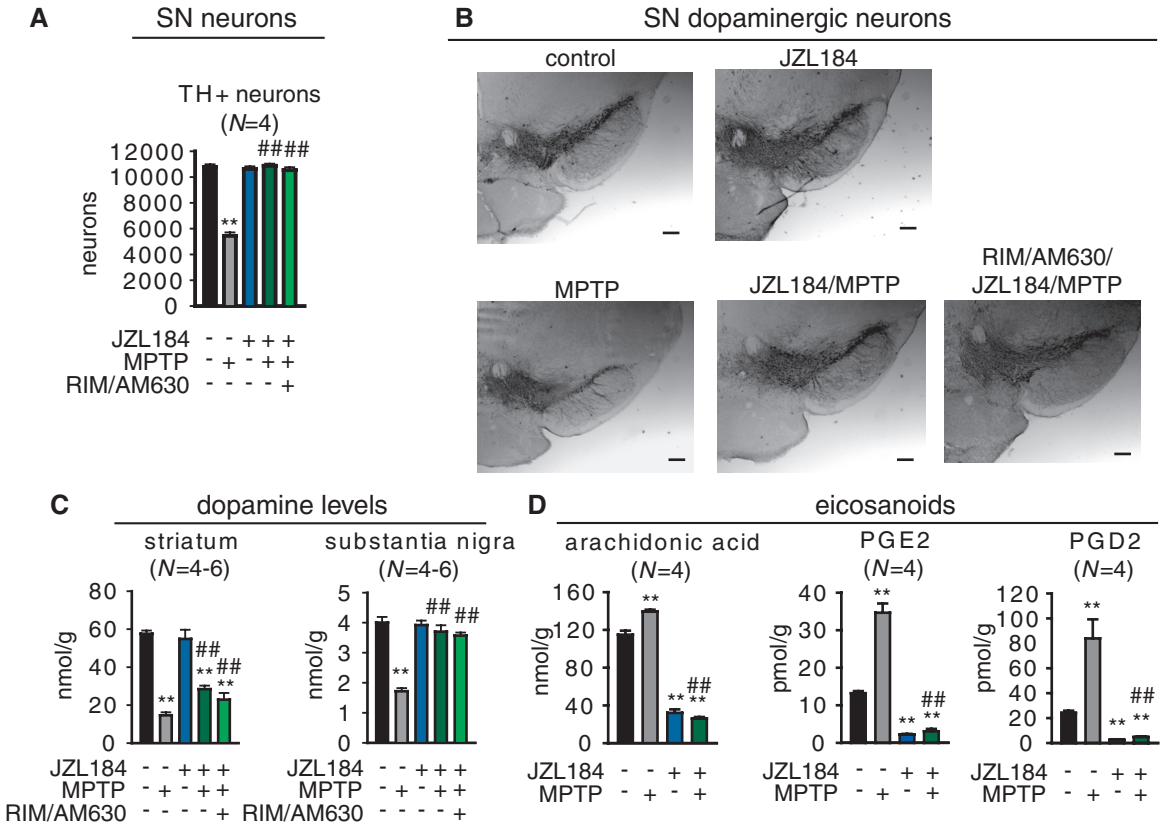

Fig. 4. MAGL blockade protects against MPTP-induced dopaminergic neurodegeneration. (**A**) Number of dopaminergic neurons as measured by counting tyrosine hydroxylase (TH)–positive cells in the substantia nigra of JZL184-treated (40 mg/kg oral gavage; daily treatment starting 1 day before MPTP administration) versus vehicle-treated mouse groups. AM630/rimonabant (formulated together, 10 mg/kg, oral gavage) was administered 30 min before JZL184 treatments. (**B**) Representative images of the substantia nigra of JZL184-, AM630/rimonabant/JZL184- versus vehicle-treated mouse groups. Neurons were detected by TH staining of fixed sections of the substantia nigra. Images were taken at 4× with a bright-field microscope. Panels in (B) are the same magnification; scale bars, 200 μm. (**C**) Dopamine levels as measured by LC-MS in the striatum and substantia nigra of JZL184- versus vehicle-treated mouse groups. (**D**) Whole-brain eicosanoid levels from JZL184- versus vehicle-treated mouse groups. MPTP treatment consisted of four doses of 15 mg/kg i.p. every 2 hours. Eicosanoid levels were measured 1 day after initial MPTP treatments. Dopaminergic neuron count and images and dopamine levels were obtained 7 days after initial MPTP treatments. $^{**}P < 0.01$ for all groups compared with vehicle-treated control mice. $^{\#\#}P < 0.01$ for all JZL184-treated MPTP groups versus vehicle-treated MPTP groups. Data are means ± SEM; $N = 4$ to 6 mice per group. Experiments were performed twice, and one representative data set is shown.

regulated these lipids in gut and spleen (Fig. 3, D and E). We also found that elevations in proinflammatory cytokines were significantly blunted in lung and liver tissue from LPS-treated *Mgll*$^{-/-}$ mice (fig. S8, A and B). Neither MAGL nor cPLA$_2$ made a substantial contribution to prostaglandin production in heart or kidney (fig. S8, C and D), where distinct PLA$_2$s (*26*) may regulate eicosanoid metabolic pathways. These findings reveal a clear anatomical segregation for the enzymatic pathways that supply the AA precursor of proinflammatory prostaglandins, and further, they suggest that MAGL inactivation may avoid some of the major adverse pharmacological effects of COX inhibitors (*7*). Prominent among the toxicities caused by COX inhibitors is gastrointestinal bleeding (*7*). Consistent with our finding, JZL184 does not cause the gastric hemorrhaging that is observed with COX1 or dual COX inhibitors (fig. S9). On the contrary, recent data suggest that inhibition of MAGL by JZL184 exerts a CB1 receptor–dependent protective effect on COX inhibitor–induced gastric bleeding (*27*).

Many neurodegenerative disorders involve a strong inflammatory component (*1*). We tested the effects of MAGL blockade in the 1-methyl-4-phenyl-1,2,3,6-tetrahydropyridine (MPTP) mouse model of Parkinsonism, in which COX inhibitors are known to be neuroprotective (*4*). Indeed, neuroprotection could be partly due to blocking PGE$_2$ production, which is toxic to dopaminergic neurons (*28*). We found that either pharmacologic (JZL184, 40 mg/kg, oral treatment once per day starting 24 hours before MPTP treatment) or genetic inactivation of MAGL prevented MPTP-induced dopaminergic neuronal loss in the substantia nigra (Fig. 4, A and B, and fig. S10, A and B) and significantly attenuated dopaminergic neuronal terminal loss (fig. S10C) and dopamine reductions in both the substantia nigra and striatum (Fig. 4C and fig. S10D). These neuroprotective effects were accompanied by a blockade of MPTP-induced increases in brain AA, prostaglandins (Fig. 4D and fig. S10E), and proinflammatory cytokines (fig. S10F). MPTP treatment also led to elevations in brain 2-AG, which is a likely source for the MAGL-dependent increases in AA and prostaglandins (fig. S10G). Although cannabinoid agonists have previously been shown to protect against neurodegeneration in the MPTP model (*29*), the effects of MAGL blockade were not reversed by cannabinoid receptor antagonists (Fig. 4, A to C, and fig. S10H), and were recapitulated by COX inhibition (fig. S10). Pharmacological or genetic disruption of MAGL did not affect the metabolism of MPTP to 1-methyl-4-phenylpyridinium (MPP+) (fig. S11). We conclude that the neuroprotective effects of MAGL inactivation are primarily due to reductions in AA and proinflammatory prostaglandins rather than augmentation of endocannabinoid signaling.

Mammals have multiple COX enzymes (COX1 and COX2) (*3*) that produce prostaglandins, and the functional characterization and selective targeting of these enzymes have led to drugs for treating pain disorders (*2*, *3*). Here, we show that a similar diversification exists for the enzymatic sources of AA coupled to prostaglandin production, which extend beyond PLA$_2$ cleavage of phospholipids to include MAGL hydrolysis of the endocannabinoid 2-AG. This upstream branch point demarcates the anatomy of prostaglandin signaling in vivo, with MAGL exerting principal control over the tone and overall abundance of AA and prostaglandins in the brain and select peripheral tissues under both basal and inflammatory states. This discovery has translational implications in that we, and others, have found that neuroinflammatory prostaglandins derive in large part from COX1 (*2*, *20*), which also produces these signaling lipids in the gut to protect against gastrointestinal damage (*8*). That cPLA$_2$, rather than MAGL, provides the AA for prostaglandin biosynthesis in the gut suggests that MAGL inhibitors should avoid the gastrointestinal toxicity observed with COX1 inhibitors, a premise supported by our data (fig. S9). MAGL inhibitors, on the other hand, have been shown to downregulate CB1 receptors in specific brain regions and to cause mild physical dependence after chronic treatment at high doses (*12*). These adaptations will need to be considered when judging the translational potential of MAGL as a target for neuroinflammatory and neurodegenerative disorders.

References and Notes

1. C. K. Glass, K. Saijo, B. Winner, M. C. Marchetto, F. H. Gage, *Cell* **140**, 918 (2010).
2. C. A. Rouzer, L. J. Marnett, *J. Lipid Res.* **50**, S29 (2009).
3. D. L. Simmons, R. M. Botting, T. Hla, *Pharmacol. Rev.* **56**, 387 (2004).
4. P. Teismann *et al.*, *Proc. Natl. Acad. Sci. U.S.A.* **100**, 5473 (2003).
5. S. H. Choi, F. Bosetti, *Aging (Albany, N.Y.)* **1**, 234 (2009).
6. A. C. McKee *et al.*, *Brain Res.* **1207**, 225 (2008).
7. S. C. Ng, F. K. L. Chan, *Curr. Opin. Gastroenterol.* **26**, 611 (2010).
8. T. Grosser, S. Fries, G. A. FitzGerald, *J. Clin. Invest.* **116**, 4 (2006).
9. M. W. Buczynski, D. S. Dumlao, E. A. Dennis, *J. Lipid Res.* **50**, 1015 (2009).
10. T. A. Rosenberger, N. E. Villacreses, M. A. Contreras, J. V. Bonventre, S. I. Rapoport, *J. Lipid Res.* **44**, 109 (2003).
11. J. Z. Long *et al.*, *Nat. Chem. Biol.* **5**, 37 (2009).
12. J. E. Schlosburg *et al.*, *Nat. Neurosci.* **13**, 1113 (2010).
13. D. K. Nomura *et al.*, *Nat. Chem. Biol.* **4**, 373 (2008).
14. T. P. Dinh *et al.*, *Proc. Natl. Acad. Sci. U.S.A.* **99**, 10819 (2002).
15. D. M. Lambert, C. J. Fowler, *J. Med. Chem.* **48**, 5059 (2005).
16. Materials and methods are available as supporting material on *Science* Online.
17. We found that MAGL similarly regulates brain AA and prostaglandin levels in mice killed by decapitation (Fig. 1) or head-focused microwave irradiation (fig. S2), although the absolute levels of AA and eicosanoids were 1/5th to 1/20th those in microwaved brains (fig. S2B). Microwaving as a method has been introduced to minimize post mortem accumulation of AA and prostaglandin lipids in brain tissue (*31*, *32*). Our data might therefore suggest that MAGL regulates both basal and ischemic pools of brain eicosanoids; however, we also evaluated brains that were removed from mice after decapitation and left to sit at room temperature for 20 min before processing and found that MAGL did not regulate the dramatic increases in AA and prostaglandins that were observed in these brain samples (fig. S2). These data thus indicate that MAGL does not control the major ischemia-induced pools of AA and prostaglandins that are known to accumulate in post mortem brain tissue (*31*, *32*). Unless otherwise noted, the studies reported herein were performed with mice killed by decapitation, which permitted parallel analysis of lipid levels and other biochemical parameters (e.g., enzyme activities and cytokine levels) that might otherwise be perturbed by brain microwaving.
18. O. Takeuchi, S. Akira, *Cell* **140**, 805 (2010).
19. B. García-Bueno, J. Serrats, P. E. Sawchenko, *J. Neurosci.* **29**, 12970 (2009).
20. S. H. Choi, R. Langenbach, F. Bosetti, *FASEB J.* **22**, 1491 (2008).
21. S. Aid, R. Langenbach, F. Bosetti, *J. Neuroinflammation* **5**, 17 (2008).
22. A. Sapirstein *et al.*, *Am. J. Physiol. Regul. Integr. Comp. Physiol.* **288**, R1774 (2005).
23. J. V. Bonventre *et al.*, *Nature* **390**, 622 (1997).
24. R. O. Sanchez-Mejia *et al.*, *Nat. Neurosci.* **11**, 1311 (2008).
25. J. V. Bonventre *et al.*, *Nature* **390**, 622 (1997).
26. G. Lambeau, M. H. Gelb, *Annu. Rev. Biochem.* **77**, 495 (2008).
27. S. G. Kinsey *et al.*, *J. Pharmacol. Exp. Ther.* **338**, 795 (2011).
28. E. Carrasco, D. Casper, P. Werner, *J. Neurosci. Res.* **85**, 3109 (2007).
29. D. A. Price *et al.*, *Eur. J. Neurosci.* **29**, 2177 (2009).
30. C. A. Smith, E. J. Want, G. O'Maille, R. Abagyan, G. Siuzdak, *Anal. Chem.* **78**, 779 (2006).
31. S. E. Farias *et al.*, *J. Lipid Res.* **49**, 1990 (2008).
32. M. Y. Golovko, E. J. Murphy, *J. Lipid Res.* **49**, 893 (2008).

Acknowledgments: We thank the members of the Cravatt laboratory for helpful discussion and critical reading of the manuscript. This work was supported by the NIH (DA017259 (B.F.C.), K99DA030908, R00DA030908 (D.K.N.), 5P01DA009789 and P01DA01725 (A.H.L.), AG028040 (B.C. and B.E.M.), R03DA027936 (M.C.G.M.), DA026261 (J.L.B.), and T32DA007027 (S.G.K.); Institute for Drug and Alcohol Studies at Virginia Commonwealth University; the Ellison Medical Foundation; and the Skaggs Institute for Chemical Biology. A patent has been filed (U.S. Patent Application no. 12/998,642) "Methods and compositions related to targeting monoacylglycerol lipase," which relates to inhibitors of monoacylglycerol lipase and associated methods, compositions, and potential uses for treating human disorders that are associated with endocannabinoid signaling. Authors who are listed inventors are J.Z.L., D.K.N, and B.F.C. The data reported in this paper are tabulated in the main text and supporting online material. Author contributions: D.K.N. and B.F.C. wrote the paper; D.K.N., B.E.M., J.L.B., S.G.K., M.C.G.M., and A.M.W. performed experiments; J.Z.L. provided reagents; and D.K.N., B.F.C., B.C., and A.H. conceived and planned experiments.

Supporting Online Material

www.sciencemag.org/cgi/content/full/science.1209200/DC1
Materials and Methods
Figs. S1 to S11
Table S1
References (*33*–*42*)

1 June 2011; accepted 23 September 2011
Published online 20 October 2011;
10.1126/science.1209200